Comparative assessment of DMT-based and CPT-based transformation models for the estimation of shear wave velocity: a case study in central Italy

Marco Uzielli[1,2#], *Diego* Marchetti[3] and *Sara* Amoroso[4,5]

[1]*Università degli Studi di Firenze, Dip. di Ingegneria Civile e Ambientale, Via di Santa Marta 3, 50139 Firenze, Italy*
[2]*Georisk Engineering S.r.l., Piazza Fra' Girolamo Savonarola 11, 50132 Firenze, Italy*
[3]*Studio Prof. Marchetti, Via Bracciano 38, 00189 Roma, Italy*
[4]*Università degli Studi di Chieti-Pescara, Viale Pindaro 42, 65129 Pescara, Italy*
[5]*Istituto Nazionale di Geofisica e Vulcanologia, Viale Crispi 43, 67100 L'Aquila, Italy*
[#]*Corresponding author: marco.uzielli@unifi.it*

ABSTRACT

The definition of the shear wave velocity profile is a fundamental step for the seismic characterization of a site in the context of Eurocode 8 and for the conduction of earthquake geotechnical engineering efforts such as site response analysis. Shear wave velocity profiles can be obtained: (1) directly from seismic geophysical and seismic geotechnical tests; or (2) indirectly, from "static" in-situ geotechnical tests such as dilatometer tests (DMT) and cone penetration tests (CPT). In the latter approach, shear wave velocity is estimated by using transformation models which are typically derived from data collected at other sites. This paper illustrates the procedures and main results of the comparative assessment of the performance of existing DMT-based and CPT-based transformation models to estimate shear wave velocity at two adjacent spatial locations in a rural site in the region of Tuscany in central Italy. Model-predicted shear wave velocity profiles were compared with direct measurements obtained by geophysical seismic dilatometer (SDMT) testing. The comparative assessment involved the definition, calculation, and assessment of quantitative performance statistics. The paper provides a critical analysis and a discussion of the outcomes with respect to soil type.

Keywords: earthquake geotechnics; shear wave velocity; cone penetration testing; dilatometer testing.

1. Introduction

The propagation velocity of shear waves V_S is a fundamental parameter for many earthquake geotechnical applications including seismic site response analyses (e.g., Choi & Stewart 2005), seismic microzonation (e.g., Martìnez-Pagan et al. 2014, Fabozzi et al. 2021), and liquefaction susceptibility analyses (e.g., Andrus et al. 2004, Amoly et al. 2016, Rahmanian & Resaie 2017, Kamel & Sbartai 2020). In static conditions, V_S has been related to the prediction of settlement in sands (e.g., Lehane & Fahey 2004), the prediction of the load-settlement behavior of shallow footings (e.g., Elhakim & Mayne 2006), the evaluation of axial elastic pile response (e.g., Mayne & Niazi 2014), and foundation design (e.g., Poulos 2022). Shear wave velocity can be correlated with many other geotechnical parameters (e.g., Hussien & Karray 2016, L'Heureux & Long 2016, Moon & Ku 2016), and can also be used to assess the level of disturbance in a soil sample (e.g., Sasitharan et al. 2011).

Shear wave velocity may be measured in laboratory (for a wide range of strain levels) and in-situ (at very small strains only). Direct in-situ measurements of V_S can be obtained from non-intrusive surface geophysical tests or through intrusive seismic tests such as down-hole testing, cross-hole testing, seismic cone penetration testing (SCPT), and seismic dilatometer testing (SDMT). Laboratory-based and geophysical methods for shear wave velocity estimation are not addressed in this paper.

Extensive research has been ongoing since the 1980's to develop correlations between V_S and results of standard, non-seismic tests such as cone penetration test (CPT), standard penetration test (SPT), and dilatometer test (DMT) among others (e.g. Marchetti et al. 2008, Amoroso 2014, Fabbrocino et al. 2015, Akin et al. 2019, Ferreira et al. 2020, Alvarez et al. 2022). SPT-based correlations are not addressed in this paper. Although direct in-situ measurements of V_S are more accurate than values estimated from indirect approaches, the latter may provide estimates of V_S in past test sites where direct S-wave measurements were not performed or where their execution is very challenging, such as deep offshore sites.

The availability of direct V_S measurements and paired results of static tests (DMT, CPT, SPT, etc.), i.e., values obtained at the same depths in proximal verticals, enables the development and calibration of correlations for the estimation of V_S itself. The extensive and increasing diffusion of probes combining static measurements and direct V_S measurements such as SDMT and SCPT extends the available dataset considerably, contributing to progressive refinements of such correlations. Moreover, the pairing procedure is beneficial in terms of the reduction of measurement uncertainty.

This paper illustrates and discusses the results of the comparative assessment of the performance of CPT-based and DMT-based transformation models for the estimation of shear wave velocity.

2. Description of the site

The geotechnical site characterization at the "I Bandi" site was conducted preliminarily in the context of a structural renovation and seismic retrofitting system for a privately owned rural building. The characterization process relied on a small-scale but rationally planned testing campaign involving a borehole, a variety of in-situ (seismic dilatometer, piezocone, dynamic penetrometer super heavy, plate load) and laboratory (index properties, direct shear, triaxial compression, oedometer, resonant column, cyclic torsional shear) geotechnical testing as well as geophysical tests (MASW, down-hole seismic refraction, electric tomography). The borehole revealed a stratigraphic profile including a surficial, cemented gravelly conglomerate underlain by silty sands and, at greater depths, interbedded layers of silty clays and clays. Among the in-situ tests comprising the site investigation, a seismic dilatometer test (SDMT) and a piezocone test (CPTU) were conducted on two spatially very proximal verticals (1 m) to minimize the likelihood of significant horizontal spatial variability of the stratigraphic profile, thus allowing a more direct comparative estimation of geotechnical uncertainty from distinct testing methods.

3. Stratigraphic profiling

Stratigraphic profiling from in-situ testing data can be conducted by identifying depth intervals displaying homogeneous mechanical behavior. In this paper, a moving-window statistical approach proposed in Uzielli et al. (2008) is employed. This approach entails the calculation of the coefficient of variation of soil behavior classification parameters such as the CPT soil behavior classification index and the DMT material index over a moving window and identifying depth intervals with coefficients of variation below a preset threshold. Soil behavior classification parameters are discussed in the following sections.

3.1. CPT-based stratigraphic profiling

Soil behavior classification can be conducted from CPT testing data through the soil behavior classification index (e.g., Robertson 2009)

$$I_c = [(3.47 - \log_{10} Q_{tn})^2 + (\log_{10} F_r + 1.22)^2]^{0.5} \quad (1)$$

In Eq. (1), the stress-normalized friction ration is defined (in %) as

$$F_r = [f_s/q_{net}] \cdot 100 \quad (2)$$

where f_s is the field-measured sleeve friction and

$$q_{net} = q_t - \sigma_{v0} \quad (3)$$

is the net cone resistance, calculated from the corrected cone resistance

$$q_t = q_c + u_2(1 - a_c) \quad (4)$$

In Eq. (4), q_c is the measured cone resistance, u_2 is the measured pore pressure, and a_c is the equipment-specific cone factor (in the case under investigation, a_c=0.80). The stress-normalized cone resistance can be calculated as

$$Q_{tn} = [q_{net}/p_a](p_a/\sigma'_{v0})^n \quad (5)$$

where σ'_{v0} is the vertical effective stress, p_a is the atmospheric pressure, and

$$q_{net} = q_t - \sigma_{v0} \quad (6)$$

is the net cone resistance, calculated from the corrected cone resistance

$$q_t = q_c + u_2(1 - a_c) \quad (7)$$

and n is a variable stress exponent which can be calculated iteratively from I_c (and Q_{tn}) as

$$n = 0.381(I_c) + 0.05(\sigma'_{v0}/p_a) - 0.15 \quad (8)$$

as suggested in Robertson (2009). The approximate boundary between sand-like and clay-like behavior is around I_c=2.60. Drained behavior can be expected for I_c<2.60. Partially drained behavior can be expected in the range 2.05≤I_c≤2.60, while I_c>2.60 likely corresponds to undrained behavior. However, the boundary at I_c=2.60 can be opportunely moved from 2.4 to 2.8 in agreement with the soil behavior properties according to Idriss and Boulanger (2014).

3.2. DMT-based stratigraphic profiling

Soil behavior classification can be pursued from DMT testing using the classification system proposed by Marchetti & Crapps (1981) and shown in Fig. 1. For soils having a dilatometer modulus E_D>1.2 as is the case for all measurements at the "I Bandi" site, soil behavior classification can be conducted by referring to the material index I_D, calculated from the corrected readings p_0 and p_1 and the hydrostatic pore pressure u_0 as

$$I_D = \frac{p_1 - p_0}{p_0 - u_0} \quad (9)$$

More specifically, I_D<0.6 can be associated with cohesive-behavior soils, 0.6≤I_D≤1.8 refers to intermediate-behavior soils, and I_D>1.8 corresponds to cohesionless-behavior soils. The approximate boundary between sand-like and clay-like behavior is around I_D=1.0 according to Robertson (2009). However, also for DMT the I_D boundary can be opportunely moved from 1.0 to 1.2 in agreement with the soil behavior properties.

3.3. Comparative assessment of soil behavior classification

Fig. 2 plots the comparative depth-wise assessment of soil behavior classification from DMT and CPT testing for the two adjacent sounding verticals as given by the soil behavior classification parameters I_D and I_c, respectively. CPT- and DMT-based classifications between cohesive-behavior (COH), intermediate-behavior (INT), and cohesionless-behavior (CHL) soils are overwhelmingly coincident along the vertical. Given the proximity of the locations, the limited differences in soil behavior classification can be ascribed to the unavoidable degree of approximation in the classification schemes and in the subjectivity of the boundary values set for the parameters I_D and I_c in the classification systems themselves.

4. Estimation of shear wave velocity

4.1. Direct estimation by seismic testing

The shear wave velocity values in the dataset were obtained with the SDMT instrumentation, which provides a direct measurement in terms of its basic definition (i.e., space divided by time). Details on SDMT testing are available in Marchetti et al. (2008) and ASTM D7400/D7400M-19 (2019).

4.2. CPT-based indirect estimation

A vast corpus of correlations is available in the geotechnical literature (e.g., Baldi et al. 1989, Robertson 1990, Rix & Stokoe 1991, Hegazy & Mayne 1995, Mayne & Rix 1995, Mayne 2006, 2007, Andrus et al.

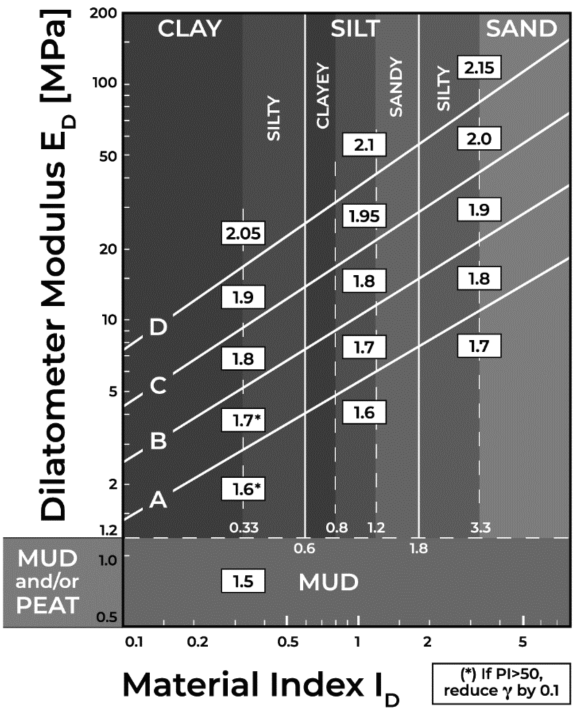

Figure 1. DMT-based soil classification chart (adapted from Marchetti & Crapps 1981)

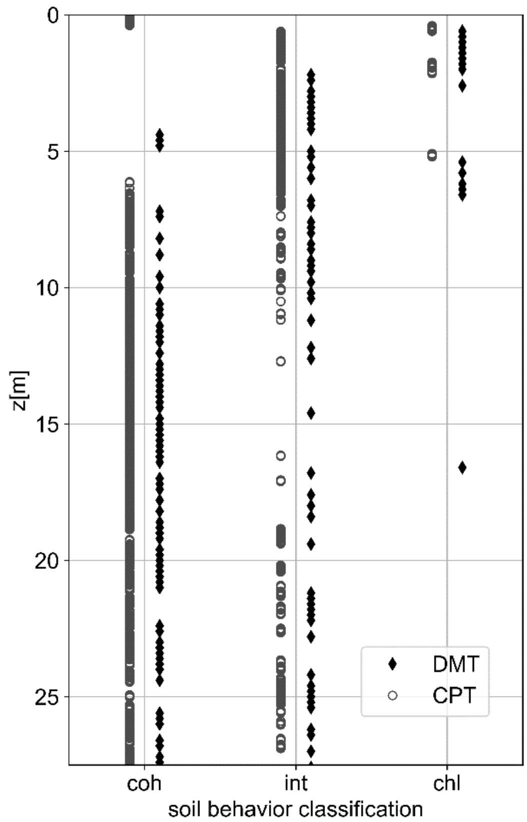

Figure 2. Depth-wise soil behavior classification from CPT and DMT data

2007, Robertson 2009, McGann et al. 2018 among others). However, most of these were developed for specific types of soils or for specific sites or regions. Wair et al. (2012) assessed comparatively the performance of numerous CPT-based V_S estimation methods and recommended the use of the following four due to their overall precision, accuracy, and breadth of applicability.

The model proposed by Hegazy & Mayne (1995), hereinafter "HM95", is valid for all soil types:

$$V_S = [10.1\log_{10}(q_t) - 11.4]^{1.67} \cdot \left[\frac{f_s}{q_t} \cdot 100\right] \tag{10}$$

where V_S is in m/s, f_s is the sleeve friction, expressed in the same units as q_t, σ_v, and P_a. Mayne (2006) proposed the following correlation (hereinafter "Ma06") based solely on sleeve friction:

$$V_S = 118.8\log_{10}(f_s) + 18.5 \tag{11}$$

with V_S in m/s and f_s in kPa. Andrus et al. (2007) proposed the following relationship (hereinafter "An07"):

$$V_S = 2.27 q_t^{0.412} I_c^{0.989} z^{0.033} ASF \tag{12}$$

where q_t is in kPa, I_c is dimensionless, z is the depth below the ground surface in m, and ASF is an age scaling factor with value of 1.00 for Holocene soils, 1.22 for Pleistocene soils, and 2.29 for Tertiary soils. The correlation proposed by Robertson (2009), hereinafter "Ro09"), considers mostly uncemented deposits ranging predominantly from Holocene to Pleistocene age:

$$V_S = [\alpha_{Vs}(q_t - \sigma_v)/P_a]^{0.5} \tag{13}$$

where V_S is in m/s, q_t is the corrected cone tip resistance, σ_v is the total vertical stress, P_a is the atmospheric pressure, and

$$\alpha_{Vs} = 10^{(0.55I_c+1.68)} \tag{14}$$

where I_c is the soil behavior type index (e.g., Robertson 2009).

4.3. DMT-based indirect estimation

Marchetti et al. (2008) proposed a set of transformation models between the small-strain shear modulus G_0 (normalized by the constrained modulus M_{DMT}) and the horizontal stress index K_D (Marchetti 1980). The above correlations are to be applied as appropriate for clays, silts or sands based on the calculated value of I_D as given in Eq. (15), Eq. (16), and Eq. (17), respectively:

$$G_0/M_{DMT} = 26.177K_D{}^{-1.0066} \quad \text{for } I_D \leq 0.6 \tag{15}$$

$$G_0/M_{DMT} = 15.686K_D{}^{-0.921} \quad \text{for } 0.6 < I_D \leq 1.8 \tag{16}$$

$$G_0/M_{DMT} = 4.5613K_D{}^{-0.7967} \quad \text{for } I_D > 1.8 \tag{17}$$

The constrained modulus can be calculated as

$$M_{DMT} = R_M \cdot E_D \tag{18}$$

in which

$$R_M = 0.14 + 2.36\log_{10}K_D \tag{19}$$

for $I_D \leq 0.6$,

$$R_M = R_{M,0} + (2.5 - R_{M,0})\log_{10}K_D \tag{20}$$

with

$$R_{M,0} = 0.14 + 0.15(I_D - 0.6) \tag{21}$$

for $0.6 \leq I_D < 3$, and

$$R_M = 0.5 + 2\log_{10}K_D \tag{22}$$

for $I_D \geq 3$, with

$$R_M = 0.32 + 2.18\log_{10}K_D \tag{23}$$

for any value of I_D if $K_D > 10$ with $R_M \leq 0.85$.

The transformation model highlights the dependency of the ratio G_0/M_{DMT} from soil type (I_D) and stress history (K_D). The correlation estimates G_0, thus requiring the indirect estimation of shear wave velocity from the fundamental relationship $V_S = \sqrt{G_0/\rho}$, where the soil density ρ can be measured in the laboratory or estimated from DMT testing data using the chart in Fig. 1.

5. Comparative assessment of model performance

The predictive capability of the DMT-based Ma08 model is assessed comparatively with those of the CPT-based HM95, Ma06, An07, and Ro09 models. The comparison between model-predicted and SDMT-measured shear wave velocities was conducted by: (1) considering the nominal SDMT measurement depths; (2) for each of the SDMT measurements, calculating the average values of CPT- and DMT-model-predicted shear wave velocities using a moving window procedure with the center of the moving window coinciding (or closest to) the SDMT measurement depth and upper and lower offsets of 20cm. A total of 54 SDMT measurements (and the same number of spatially averaged predictions for each of the 5 models) were available. Of these, 37 measurements are classified as pertaining to "cohesive-behavior" (COH) soils, 16 to "intermediate-behavior" (INT) soils, and 1 to a "cohesionless-behavior" (CHL) soil according to the sample average of the CPT-based soil behavior classification index I_c. CPT-based classification was adopted because the smaller measurement interval results in a larger sample numerosity.

The comparison relies on quantitative statistical criteria; more specifically: (1) calculation of second-moment statistics; and (2) investigation on empirical cumulative distribution functions. The two criteria are applied to; (1) the prediction error ΔV_S; and (2) relative error θV_S. The first is given by

$$\Delta_{VS} = V_{S,pred} - V_{S,SDMT} \tag{24}$$

where $V_{S,pred}$ is the model-predicted shear wave velocity and $V_{S,SDMT}$ is the SDMT-measured shear wave velocity. The second is given by

$$\theta_{VS} = \Delta_{VS}/V_{S,SDMT} \tag{25}$$

Using the relative error in addition to the prediction error allows to duly account for the tendentially higher values of V_S shown by INT soils in comparison with COH soils. Negative values of Δ_{VS} and θ_{VS} correspond to underprediction while positive values correspond to overprediction. Fig.3 shows the depth-wise plots of model predictions, prediction errors Δ_{VS}, and relative errors θ_{VS}. Fig. 4 plots the probability density histograms for prediction errors Δ_{VS} and relative errors θ_{VS}.

Table 1 reports the sample mean and sample standard deviations of Δ_{VS} and θ_{VS} by prediction model and soil type. The mean provides a measure of the overall bias in model-predicted estimates while the standard deviation parametrizes the level of scatter of model estimates around the mean. The analysis is conducted for COH and INT soils due to the single SDMT measurement

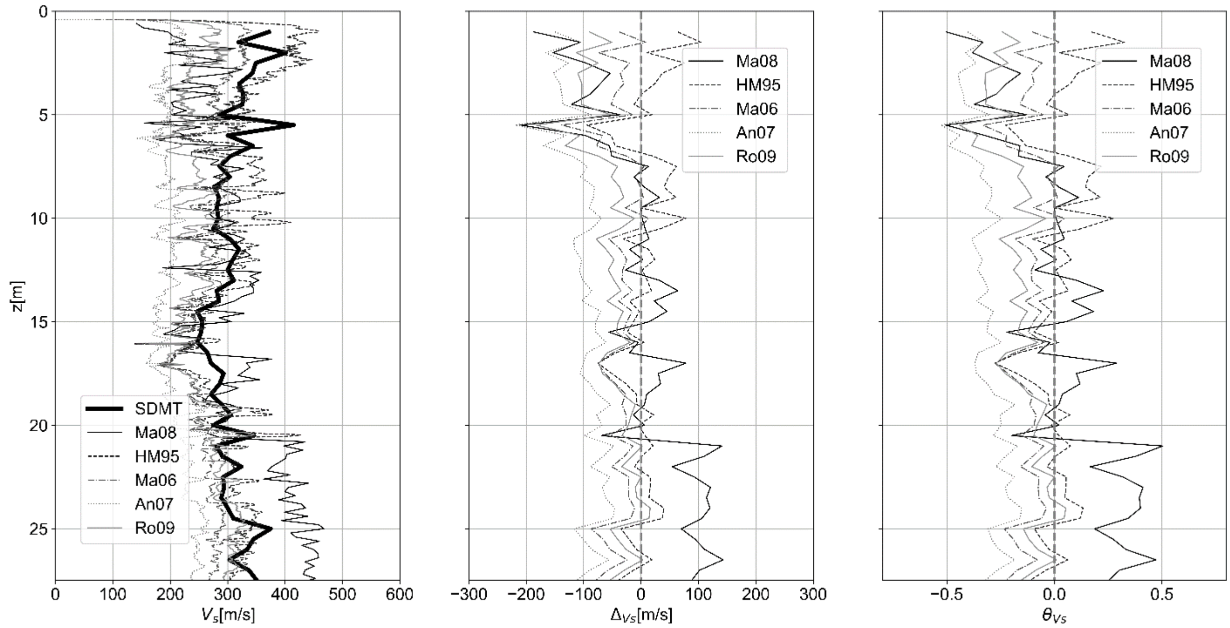

Figure 3. Depth-wise model predictions, prediction errors, and relative errors

amenable to CHL soils as discussed previously. HM95 shows the lowest bias (in absolute value) of Δ_{VS} and θ_{VS} for both COH and INT soils. Results are more articulated with respect to standard deviations: An07 shows the lowest value for both COH and INT soils for Δ_{VS}, while Ma06 shows the lowest values for θ_{VS} for both COH and INT soils.

While second-moment statistics are useful in providing an objective perspective on the performance of prediction models, supplementary considerations are warranted. From an engineering standpoint the underprediction of V_S is preferrable in most applications (e.g., seismic site response analysis), as it provides conservative estimates.

To allow a more engineering-focused comparative assessment, empirical cumulative distribution functions (ECDFs) were calculated for Δ_{VS} and θ_{VS}. These are shown in Fig. 5. The performance of the prediction models was parameterized by calculating the probability of acceptable performance as the difference between the cumulative distribution values of subjectively defined lower- and upper-bound "performance thresholds" (β_{lb} and β_{ub}, respectively):

$$\eta = ECDF(\beta_{ub}) - ECDF(\beta_{lb}) \tag{26}$$

for Δ_{VS} and θ_{VS}. This parameter provides the frequentist probability that a model's prediction can be considered reliable (in terms of prediction capability) and useful (in avoiding overestimation) from an engineering perspective. The lower- and upper-bound performance thresholds for Δ_{VS} were set at -50m/s and 0m/s, respectively, while those for θ_{VS} were set at -0.2 and 0, respectively. The above thresholds are meant to penalize overprediction and excessive underprediction error. Table 2 reports the values of η_{VS} for Δ_{VS} and θ_{VS} by prediction model and soil type. Performance thresholds are shown as dashed lines in all subplots in Fig. 5.

Ma06 and Ro09 perform significantly better than the other models in terms of $\eta(\Delta_{VS})$ for COH soils. For INT soils, however, Ro09 significantly outperforms all other models. The same patterns are noted for $\eta(\theta_{VS})$. An07 performs consistently worse than all other models and can thus be deemed to rank last in terms of engineering

Table 1. Second-moment statistics of prediction error and relative error

		Δ_{VS}		θ_{VS}	
Model	Soil type	mean [m/s]	st.dev. [m/s]	mean [m/s]	st.dev. [m/s]
Ma08	COH	33	56	0.11	0.18
	INT	-46	94	-0.13	0.28
HM95	COH	2	33	0.01	0.11
	INT	14	48	0.05	0.14
Ma06	COH	-33	29	-0.11	0.07
	INT	-38	34	-0.11	0.09
An07	COH	-89	23	-0.30	0.07
	INT	-114	44	-0.35	0.10
Ro09	COH	-39	27	-0.13	0.08
	INT	-70	48	-0.21	0.13

Table 2. Probability of acceptable performance

	$\eta(\Delta_{VS})$		$\eta(\theta_{VS})$	
Model	COH	INT	COH	INT
Ma08	0.18	0.11	0.24	0.17
HM95	0.42	0.24	0.43	0.28
Ma06	0.65	0.68	0.81	0.74
An07	0.01	0.08	0.07	0.14
Ro09	0.63	0.17	0.75	0.39

utility in this case study. It should be noted that An07 displays low standard deviations (but high mean in absolute value) in comparison with other models. HM95 had shown very low mean values of Δ_{VS} and θ_{VS}, but the high standard deviations result in a very low fraction of predictions to be "useful" on the basis of the selected performance thresholds. In other words, An07 proved to be excessively conservative for the "I Bandi" site. Most models showed a better prediction performance for COH soils than for INT soils, with respect to both Δ_{VS} and θ_{VS}. The most notable exception is given by the An07 which, however, showed the lowest performance among all models in terms of both $\eta(\Delta_{VS})$ and $\eta(\theta_{VS})$.

The DMT-based Ma08 model showed very different levels of performance depending on soil type. For COH soils, it proved to be largely unconservative, while for INT soils it was balanced in terms of conservatism vs. unconservatism. However, only 11% and 17% of the predictions fell within the acceptability range for Δ_{VS} and θ_{VS}, respectively.

6. Concluding remarks

This paper provided a case study focusing on the comparative assessment of the prediction capabilities of CPT- and DMT-based models for the estimation of shear wave velocity.

The critical analysis of model predictions highlighted the heterogeneous level of inter-method performance. Intra-method performance also varies between cohesive-behavior and intermediate-behavior soils.

It should be highlighted that the performance statistics and the associated assessments are case-specific and could ranking of prediction models may vary for other sites. Therefore, further applications would be

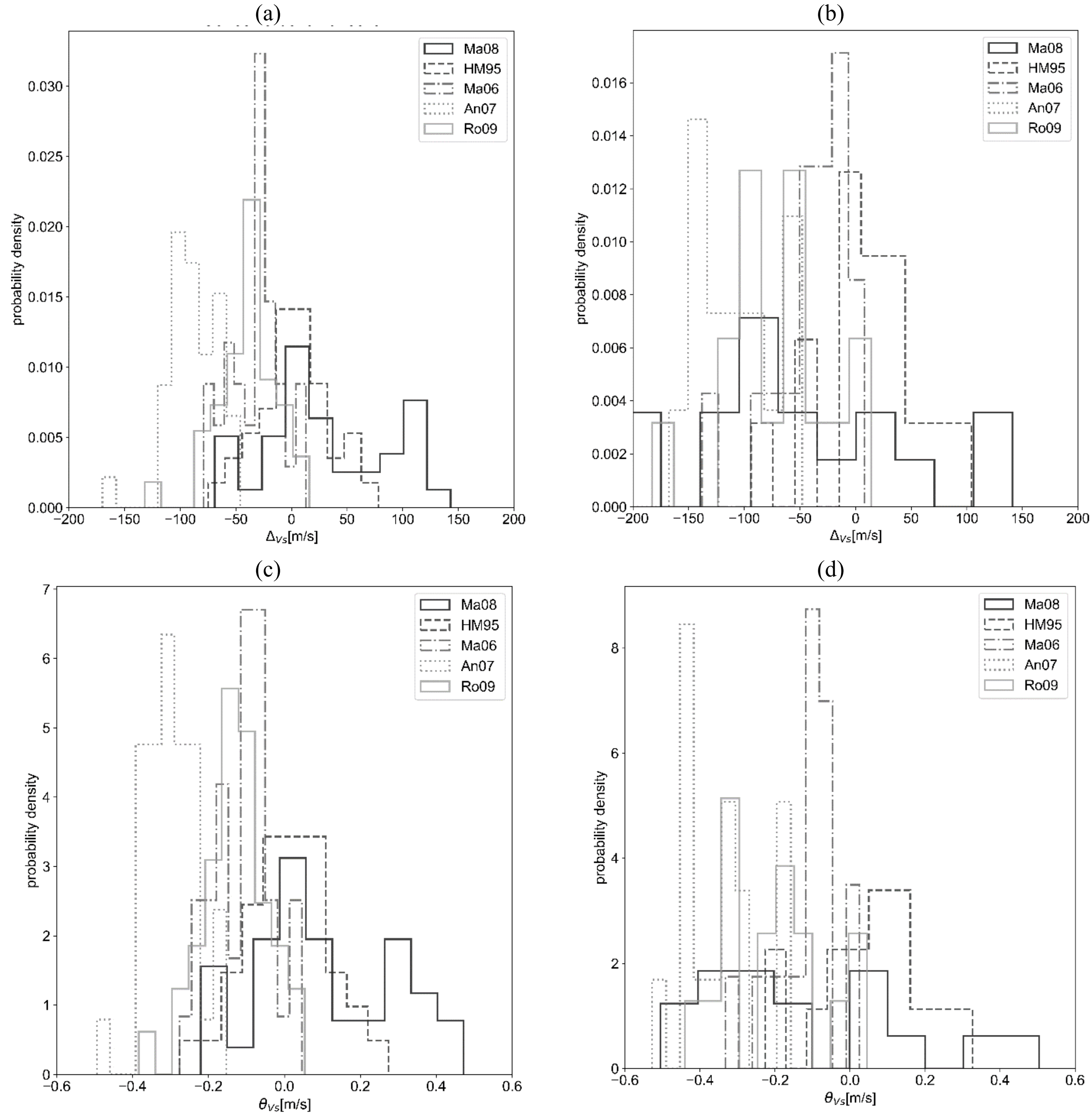

Figure 4. Probability density histograms of prediction errors and relative errors: (a) prediction error for cohesive-behavior soils; (b) prediction error for intermediate-behavior soils; (c) relative error for cohesive-behavior soils; (d) relative error for intermediate-behavior soils.

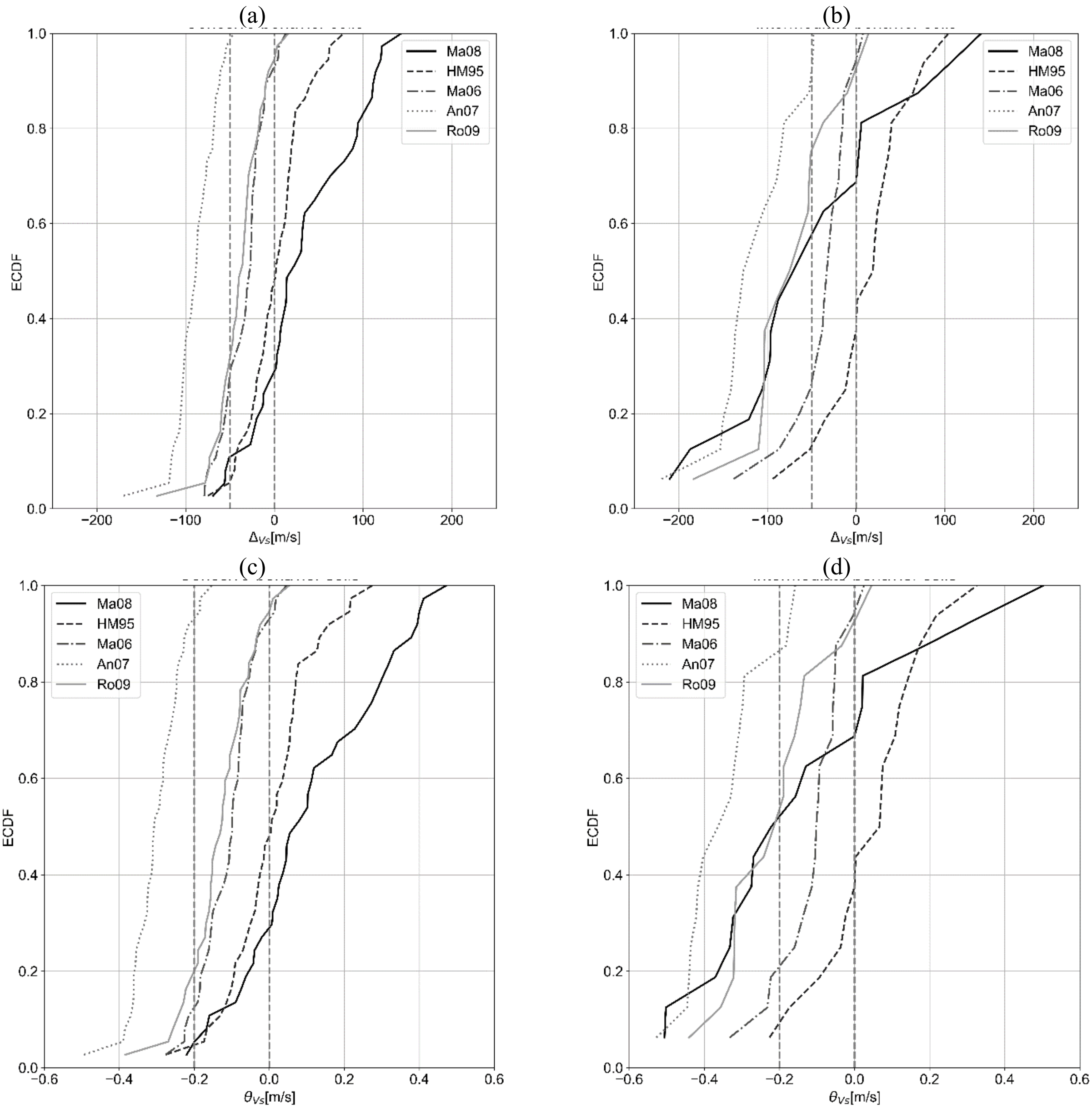

Figure 5. Empirical cumulative distribution functions for: (a) prediction error for cohesive-behavior soils; (b) prediction error for intermediate-behavior soils; (c) relative error for cohesive-behavior soils; (d) relative error for intermediate-behavior soils.

recommended at sites characterized by different geological age, cementation, soil type, effective stress state.

References

Akin, M.K., Kramer, S.L., Topal, T. "Empirical correlations of shear wave velocity (Vs) and penetration resistance (SPT-N) for different soils in an earthquake-prone area (Erbaa-Turkey)". Engineering Geology, vol. (119), pp. 1–17, 2011. https://doi.org/10.1016/j.enggeo.2011.01.007

Alvarez, B. I., Palma, H. B., Besenzon, D., Vera-Grunauer, X., Amoroso S. "Geotechnical characterization of the estuarine deltaic deposits in the Guayaquil city through in situ and laboratory tests." Soils and Rocks 45(3), e2022074021, 2022. https://doi.org/10.28927/SR.2022.074021

Amoly, R.S., Ishihara, K., Bilsel, J. "The relation between liquefaction resistance and shear wave velocity for new and old deposits." Soils Found. 56(3), pp. 506-519, 2016. https://doi.org/10.1016/j.sandf.2016.04.016.

Amoroso, S. "Prediction of the shear wave velocity Vs from CPT and DMT at research sites". Frontiers of Structural and Civil Engineering 8, pp. 83–92, 2014. https://doi.org/10.1007/s11709-013-0234-6.

Andrus, R.D., Stokoe, K.H., Juang, C.H. "Guide for Shear-Wave Based Liquefaction Potential Evaluation." Earthquake Spectra 20(2), pp. 285–308, 2004. https://doi.org/10.1193/1.1715106.

Andrus, R.D., Mohanan, N.P., Piratheepan, P., Ellis, B.S., Holzer, T.L. "Predicting shear-wave velocity from cone penetration resistance." Proc. 4th international conference on earthquake geotechnical engineering, 2007.

ASTM "ASTM D7400/D7400M-19 Standard test methods for downhole seismic testing." https://www.astm.org/Standards/D7400.htm, 2019.

Baldi, G., Bellotti, R., Ghionna, V.N., Jamiolkowski, M., Lo Presti, D.C.F. "Modulus of sands from CPTs and DMTs." Proc. 12th Inter. Conf. Soil Mech. and Foundation Eng., Vol. 1, Rio de Janeiro, pp 165-170, 1989.

Boulanger R.W., Idriss I.M. "CPT and SPT based liquefaction triggering procedure". Report No. UCD/CGM-14/01, Center for Geotechnical Modelling, Department of Civil and Environmental Engineering, Univ. California, California, 134 pp, 2014.

Choi, Y., Stewart, J.P. "Nonlinear Site Amplification as Function of 30 m Shear Wave Velocity." Earthquake Spectra 21(1), pp. 1-30, 2005. https://doi.org/10.1193/1.1856535.

Elhakim, A.F., Mayne, P.W. "Evaluating footing response from seismic piezocone tests." in Site and Geomaterial Characterization, pp. 255-260, 2006. https://doi.org/10.1061/40861(193)3.

Fabozzi, S., Catalano, S., Falcone, G., Naso, G., Pagliaroli, A., Peronace, E., Porchia, A., Romagnoli, G., Moscatelli, M. "Stochastic approach to study the site response in presence of shear wave velocity inversion: Application to seismic microzonation studies in Italy." Engineering Geology Vol. 280, http://doi.org/10.1016/j.enggeo.2020.105914, 2021.

Fabbrocino, S., Lanzano, G., Forte, G., de Magistris, F.S., Fabbrocino, G. "SPT blow count Vs. shear wave velocity relationship in the structurally complex formations of the Molise Region (Italy)". Engineering Geology, vol. 187, pp. 84–97, 2015.

Ferreira, C., Viana da Fonseca, A., Ramos, C., Saldanha, A.S., Amoroso, S., Rodrigues, C. "Comparative analysis of liquefaction susceptibility assessment methods based on the investigation on a pilot site in the greater Lisbon area. Bulletin of Earthquake Engineering 18, pp. 109-138, https://doi.org/10.1007/s10518-019-00721-1, 2020.

Hegazy Y.A., Mayne, P.W. "Statistical correlations between Vs and CPT data for different soil types." In: Proceedings of the Symposium on Cone Penetration Testing. Swedish Geotechnical Society, Linköping Vol. 2, pp. 173–178, 1995.

Hussien, M.N., Karray, M. "Shear wave velocity as a geotechnical parameter: an overview." Can. Geotech. J., vol. 53(2), pp. 252-272, 2016. https://doi.org/10.1139/cgj-2014-0524.

Kamel, F., Sbartai, B. "Liquefaction analysis using shear wave velocity." Civil Engineering Journal 6(10), pp. 1944-1955, 2020. http://doi.org/10.28991/cej-2020-03091594.

Lehane, B.M., Fahey, M. "Using SCPT and DMT data for settlement prediction in sand." In ISC-2 on Geotechnical and Geophysical Site Characterization, pp. 1673-1679, 2004.

L'Heureux, J.S., Long, M. "Correlations between shear wave velocity and geotechnical parameters in Norwegian clays." In 17th Nordic Geotechnical Meeting (NGM 2016), 2016.

Marchetti, S. "In situ tests by flat dilatometer." Journal of the Geotechnical Engineering Division, ASCE, Vol. 106(GT3), pp. 299-321, 1980.

Marchetti, S., Crapps, D.K. "Flat dilatometer manual." Internal report, GPE, 1981.

Marchetti, S., Monaco, P., Totani, G., Marchetti, D. "In Situ Tests by Seismic Dilatometer (SDMT). In: Proceedings of the From Research to Practice in Geotechnical Engineering." ASCE Geotech. Spec. Publ. No. 180 (honoring J.H. Schmertmann), pp. 292–311, 2008.

Martìnez-Pagan, P., Navarro, M., Pérez-Cuevas, J., Alcalà, F.J., Garcìa-Jeréz, A., Sandoval-Castaño, S. "Shear wave velocity based seismic microzonation of Lorca city (SE Spain) from MASW analysis." Near Surface Geophysics. http://doi.org/10.3997/1873-0604.2014032, 2014.

Mayne, P.W. "In situ test calibrations for evaluating soil parameters." Proc. Characterization and Engineering Properties of Natural Soils II, Singapore, 2006.

Mayne, P.W. "Cone penetration testing state-of-practice." NCHRP Project 20-05, Topic 37-14, 2007.

Mayne, P.W., Rix, G.J. "Correlations between shear wave velocity and cone tip resistance in natural clays." Soils and Foundations 35(2), pp. 107-110, 1995.

Mayne, P.W., Niazi, F.S. "Evaluating axial elastic pile response from cone penetration tests (The 2009 Michael W. O'Neill Lecture)." DFI J. - J. Deep Found. Inst., 2014.

McGann, C.R., Bradley, B.A., Jeong, S. "Empirical Correlation for Estimating Shear-Wave Velocity from Cone Penetration Test Data for Banks Peninsula Loess Soils in Canterbury, New Zealand." J. Geot. .Geoenv. Eng. 144(9), 2018. http://doi.org/10.1061/(ASCE)GT.1943-5606.0001926.

Moon, S.W., Ku, T. "Development of global correlation models between in situ stress-normalized shear wave velocity and soil unit weight for plastic soils." Can. Geotech. J., Vol. 53(10), pp. 1600-1611, 2016. https://doi.org/10.1139/cgj-2016-0015.

Poulos, H.G. "Use of shear wave velocity for foundation design." Geotechnical and geological engineering 4, 2022. http://doi.org/ 10.21203/rs.3.rs-493427/v1.

Rahmanian, S., Rezaie, F. "Evaluation of liquefaction potential of soil using the shear wave velocity in Tehran, Iran." Geosciences Journal 21, pp. 81-92, 2017. https://doi.org/10.1007/s12303-015-0039-9.

Rix, G.J., Stokoe, K.H. "Correlation of initial tangent modulus and cone penetration resistance." Calibration Chamber Testing, (Proc. ISOCCT, Potsdam), Elsevier Publishing, New York, pp. 351-362, 1991.

Robertson, P.K. "Soil classification using the cone penetration test." Canadian Geotechnical Journal 27(1), pp. 151-158, 1990. https://doi.org/10.1139/t90-014.

Robertson, P.K. "Interpretation of cone penetration tests — a unified approach," Canadian Geotech. J. 46(11), pp. 1337-1355, 2009. https://doi.org/10.1139/T09-065.

Sasitharan, S., Robertson, P.K., Sego, D. (2011). "Sample disturbance from shear wave velocity measurements." Canadian Geotechnical Journal 31(1), pp. 119-124. http://doi.org/10.1139/t94-013.

Uzielli, M., Simonini, P., Cola, S. (2008). Statistical identification of homogeneous soil layers in Venice lagoon soils. Geotechnical and Geophysical Site Characterization - Proceedings of the 3rd International Conference on Site Characterization ISC'3, Taipei, April 1-4, 2008. The Netherlands: Taylor & Francis, ISBN: 9780415469364.

Wair, B.R., DeJong, J.T., Shantz, T. (2012). "Guidelines for Estimation of Shear Wave Velocity Profiles." Pacific Earthquake Eng. 8, p. 68.